

# Device for frequency chirp measurements of optical transmitters in real time

Tapio Niemi<sup>a)</sup>

*Fiber-Optics Group, Metrology Research Institute, Helsinki University of Technology, P.O. Box 3000, FIN-02015 HUT, Finland*

Simo Tammela<sup>b)</sup>

*VTT Electronics, Microelectronics, P.O. Box 1101, FIN-02044 VTT, Finland*

Hanne Ludvigsen

*Fiber-Optics Group, Metrology Research Institute, Helsinki University of Technology, P.O. Box 3000, FIN-02015 HUT, Finland*

(Received 5 July 2001; accepted for publication 17 December 2001)

We present a new automated device for measurement of time-resolved frequency chirp of optical transmitters. It measures chirp in real time by utilizing two temperature-tunable silicon-wafer etalons as frequency discriminators. The time-resolved frequency chirp in a range of  $\pm 12$  GHz can be measured with a time resolution of approximately 40 ps. © 2002 American Institute of Physics. [DOI: 10.1063/1.1448898]

## I. INTRODUCTION

Directly modulated distributed feedback lasers are widely used in metropolitan area and access networks as a cost-efficient solution for the optical transmitter. Utilization of these lasers in systems with long optical fibers is, however limited due to the frequency fluctuations induced by the direct modulation of the laser current. The current modulation induces changes in the refractive index of the laser, which lead on to changes of the frequency of the light emitted by the laser. This frequency variation is commonly referred to as frequency chirp. Interaction of the frequency chirping with chromatic dispersion in the optical fiber distorts the transmitted signal and results in dispersion penalty. In modern metropolitan area networks, the length of the optical fiber may be on the order of a few hundred kilometers, which means that dispersion-induced problems remain an important issue.

The performance of an optical communication system is characterized by the bit-error ratio (BER). The effect of chirping and dispersion are observed as a dispersion penalty in the BER measurement. A drawback with the BER measurements is that in order to obtain reliable results the measurement has to be extended over a long time interval. Since the measurement of the frequency chirp can be made fast, it could serve as a simple test to estimate the performance of the directly modulated laser in real networks.

Several methods have been implemented to characterize frequency chirping of modulated light sources. For instance, a transfer function taking the dispersion of the fiber into account can be used to evaluate the magnitude of the chirp.<sup>1-4</sup> However, this method does not allow for time-resolved measurements of the chirp, which is important for accessing information about the frequency variations within individual

pulses. The time-resolved chirping characteristics of directly modulated lasers have been measured using a narrowband tunable optical filter to map out the spectrum of the transmitter in time.<sup>5,6</sup> From these measurements it is possible to calculate the variations in the optical frequency as a function of time. This measurement takes a relatively long time, since a large number of filter settings are needed. If the light source has a narrow spectral width, it is sufficient to know the variation of only the center frequency when the intensity is modulated. In this case, a frequency discriminator can be utilized to transfer the fluctuations of the optical frequency into intensity variations.<sup>7,8</sup> To allow for the frequency chirp to be extracted from the amplitude-modulated signal, two successive measurements with different settings of the discriminator are needed. Consequently, the method is not suited for monitoring the frequency chirp in real time. Recently, a waveguide grating router was used for such a real-time measurement of the frequency chirp.<sup>9</sup> This device, however, operates only in a single wavelength at a time and tuning to another wavelength is slow.

In this article, we present a new method to measure time-resolved frequency chirp in real time. We have previously demonstrated that a silicon-wafer etalon can conveniently be used as a frequency discriminator.<sup>10,11</sup> The etalon allows operation over a broad wavelength range, from 1.1  $\mu\text{m}$  to 1.7  $\mu\text{m}$ , and tuning to another wavelength is simple and fast. Our new device is based on the use of two such etalons. The measurement system is fully automated, which is important for fast characterization of laser transmitters.

## II. TEMPERATURE-TUNABLE ETALON MADE OF SILICON

In the near infrared region, a solid etalon made of silicon offers many attractive features for realizing an optical resonator in a compact and cost-effective format. Silicon is trans-

<sup>a)</sup>Electronic mail: tapio.niemi@hut.fi

<sup>b)</sup>Present address: Liekki Ltd., Sorronrinne 9, FIN-08500, Lohja.

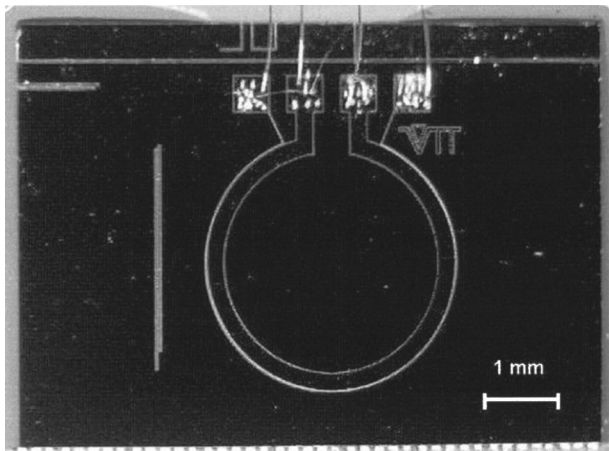


FIG. 1. Silicon chip with integrated heating and sensing resistors.

parent for wavelengths in the range of  $1.1 \mu\text{m}$  to  $40 \mu\text{m}$  and the absorption coefficient is small. Furthermore, the processing techniques of silicon are well developed. The refractive index of silicon exhibits a strong dependence on temperature, since the absorption edge is close to the wavelengths of interest. The position of the absorption edge changes with temperature and, therefore, according to the Kramers–Kronig relations the refractive index is also varied.<sup>12</sup> The optical thickness of the etalon may thereby conveniently be tuned by changing the index of refraction of silicon by temperature tuning.<sup>11,13</sup>

Our etalon is made of a silicon wafer polished on both sides. The polished surface acts as a relatively good mirror even without any reflective coatings due to the high index of refraction of silicon. The refractive index is 3.48 at a wavelength of  $1.55 \mu\text{m}$  and its temperature coefficient is  $\sim 1.5 \times 10^{-4}$  1/K. The coefficient of temperature expansion of silicon is two orders of magnitude smaller ( $\sim 2.5 \times 10^{-6}$  1/K), making it to have a negligible effect to the change in the optical length of the etalon when the temperature is tuned. The outlook of the silicon chip is given in the photograph of Fig. 1. The size of the chip is  $6 \text{ mm} \times 8 \text{ mm}$  and it is less than 1 mm thick. Controlling of the temperature of the chip is realized with a metal thin-film resistor integrated on the surface of the chip. A second thin-film resistor can be used for sensing the changes in the temperature of the chip, if necessary. The diameter of the ring-shaped resistor film is 3 mm, its thickness 200 nm and its resistance  $\sim 35 \Omega$ . The resistors are fabricated by sputtering molybdenum onto the surface of the chip. The heating of the chip is realized simply by feeding current through the resistor.

### III. FABRY–PEROT ETALON AS THE FREQUENCY DISCRIMINATOR

To be able to use the Fabry–Perot (FP) etalon in a fiber-optic system, we inserted it in a 25 mm airgap of a commercial fiber-optic beam expander (JDS FBOB30-FPPF). The light passes through the etalon in the center of the ring-shaped heating resistor at close to normal incidence, at which the transmission of the etalon is polarization insensitive.<sup>10</sup> The transmission spectrum of the silicon etalon was deter-

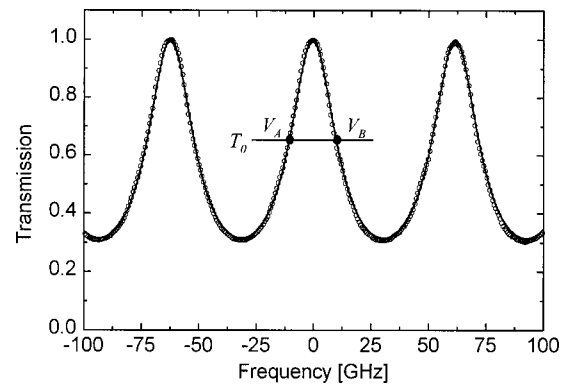


FIG. 2. Measured (open circles) and fitted (solid line) transmission spectrum of the silicon etalon.

mined by applying broadband spontaneous emission from an erbium-doped fiber amplifier. The signal passing through the etalon was measured with an optical spectrum analyzer and the transmission spectrum was fitted to the Airy function. The measured (open circles) and the fitted (solid line) curves are given in Fig. 2.

The transmission spectrum exhibits periodical fringes whose distance determines the free spectral range (FSR) of the etalon. The slope of the transmission fringe works efficiently as a frequency discriminator. The values of the FSR and the reflectivity were obtained from the fitted Airy function. Our etalon has a FSR of 62.0 GHz, which translates into a wafer thickness of  $680 \mu\text{m}$ . The reflectivity  $R$  is  $\sim 28\%$ . The frequency discrimination properties of the etalon can be varied by using wafers of different thickness and by depositing dielectric layers on the chip to act as mirror surfaces. The position of the transmission fringes shifts in frequency as the temperature of the etalon is tuned. We have measured the shift in the fringe position to be  $\sim 11 \text{ GHz/K}$ .

Frequency chirping of the intensity-modulated signal can be determined from two successive measurements with different slopes of the frequency discriminator.<sup>7,8</sup> The measurement points are selected to coincide with the middle point on the transmission slope,  $T_0$ , defined according to the relation  $T_0 = (T_{\text{MAX}} + T_{\text{MIN}})/2$ , where  $T_{\text{MAX}}$  and  $T_{\text{MIN}}$  are the maximum and the minimum transmission of the etalon. When the optical signal containing frequency chirp passes through FP etalon, which is tuned to the slope of the transmission fringe, the etalon transmission changes with the variations of the signal frequency. When the transmission point is at the positive slope, the positive frequency changes cause an increase and negative changes a decrease in the transmission. The frequency chirp can be calculated by applying the relation<sup>10,11</sup>

$$\Delta \nu(t) \approx \frac{\text{FSR}}{2\pi} \frac{V_A(t) - V_B(t)}{V_A(t) + V_B(t)} \times \left[ (1 - T_0) \left[ T_0 \frac{(1 + R)^2}{(1 - R)^2} - 1 \right] \right]^{-1/2}, \quad (1)$$

where  $V_A(t)$  and  $V_B(t)$  are the signal wave forms measured at the positive and the negative slope, respectively. Equation (1) is an approximation, which holds for frequency chirps in

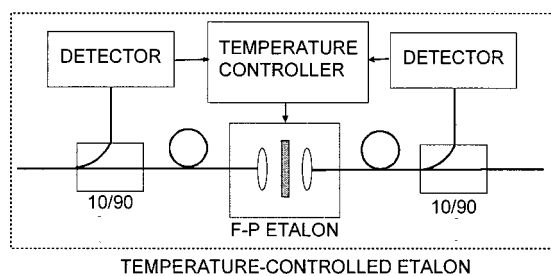


FIG. 3. Basic setup for controlling the transmission of the temperature-tunable etalon.

the range  $\Delta\nu \ll \text{FSR}/2$ . The time resolution of our etalon is approximately 40 ps allowing for frequency-chirp measurements with bit rates up to 2.5 Gbit/s. The maximum resolvable frequency deviation is  $\pm 12$  GHz. The selection of the optical properties will also involve a trade off between the frequency selectivity and the time resolution of the interferometer.

#### IV. EXPERIMENTAL SETUP FOR CHIRP ANALYSIS

To allow for automatic operation of the chirp analyzer both active monitoring and controlling of the transmission of the etalon are required. A basic setup for performing this task for one single etalon is given in Fig. 3. The transmission of the etalon is monitored by coupling out a fraction of the optical power before and after it. The average power is measured using two detectors (PDT0311) whose photocurrent is converted into voltage by using a current-to-voltage converter. This voltage is digitized with an 8-bit AD converter and the value of the transmission point is obtained by calculating the ratio of the powers detected before and after the etalon. The AD converter and the operation of the device are controlled using a microcontroller (PIC 16C74A).

The measurement with a single frequency discriminator requires the etalon to be tuned between the two operation points ( $V_A$  and  $V_B$ ), hence it does not allow for real-time detection of the frequency chirp. By using two etalons, it is possible to perform the measurements at two different slopes simultaneously. An outline of the setup for the real-time chirp analyzer is depicted in Fig. 4.

The laser transmitter was modulated in a pseudo-random-bit sequence (PRBS) using a pattern generator. The light from the optical transmitter is split with a 3 dB coupler. The two branches of the signal pass through two temperature-controlled etalons with approximately the same properties. One of them is tuned and locked to the positive

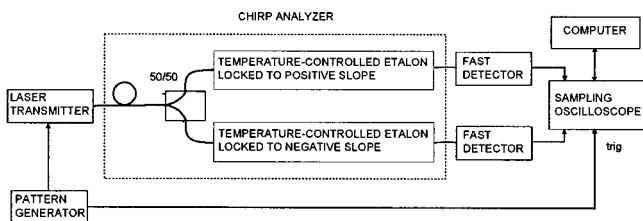


FIG. 4. Experimental setup for measurement of time-resolved frequency chirp in real time based on using two temperature-controlled etalons with similar optical properties.

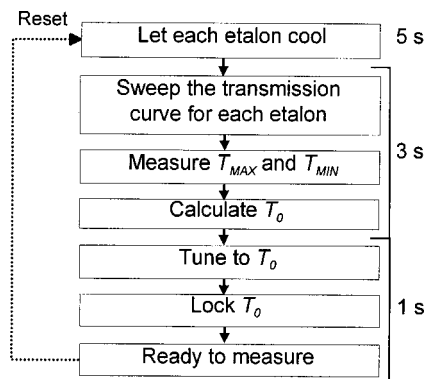


FIG. 5. Flow diagram for the measurement procedure. The time durations are given to the right.

slope of the transmission fringe of the etalon and the other to the negative slope. We used one microcontroller for each etalon to control the locking points. This allows for simultaneous measurement of both of the wave forms needed to calculate the frequency chirp of the optical signal. The wave forms after the temperature-controlled etalons were detected with fast detectors and the traces were displayed and stored on different channels of a digital-sampling oscilloscope. The oscilloscope was synchronized with a trigger signal of the pattern generator and it was controlled via a GPIB interface using a LabView program, which collects the data and performs the calculation of Eq. (1).

Before the measurement can begin the analyzer needs to be initialized. The initialization is carried out when the device is turned on or the reset command is given. A flow diagram for this procedure is depicted in Fig. 5.

First, the etalons are let to cool down close to the ambient temperature. Then, the heating power is turned on which causes the transmission fringes of the etalon to tune in frequency. During the tuning, the transmission of the etalon is monitored by detecting the optical power before and after each etalon. The transmission value is obtained by calculating the ratio of the detected powers.

The maximum,  $T_{MAX}$ , and the minimum,  $T_{MIN}$ , values are stored for determination of the operation point on the transmission fringe. The microcontroller then automatically finds the operation point  $T_0$  and locks the transmission of each etalon. One of the etalons is locked to the positive transmission slope and the other to the negative slope. The locking is realized with an adaptive digital PI algorithm. The bandwidth of the feedback signal is limited by the time needed for the silicon chip to respond to rapid changes in the heating current. The response of the chip is slow due to its relatively large size. The maximum frequency of the tuning current was measured to be  $\sim 50$  Hz, above which the etalon does not respond to the variations in the heating current. Once the etalons are locked to their respective operation points, the device is ready for performing measurements. The time required to perform one single measurement including initialization of the device is  $\sim 10$  s. Once the initialization has been executed the device can track the frequency chirp of the transmitter in real time.

The optical components of the analyzer may exhibit dif-

ferences in attenuation and in the length of the fiber pigtailed. The difference in attenuation was accounted for by measuring the ratio of the average powers of the two signals at the outputs. These powers were equalized in the computer by applying a correction factor. The difference in lengths between the two paths was adjusted by tuning both of the etalons to the same slope of the transmission fringe. In this case, the measured wave forms are almost identical. By applying a time offset between the two channels of the scope, we compensated for the difference in the arrival times of the signal pulses.

The sensitivity of the device was investigated by sinusoidally modulating the laser frequency of a tunable laser source (Photonics TUNICS-PRI) and measuring the induced frequency variation with the chirp analyzer. This investigation showed that the analyzer is capable of measuring frequency variations of less than 200 MHz reliably.

## V. CHIRP MEASUREMENTS

To test the performance of the chirp analyzer we measured the frequency chirp of a directly modulated DFB-laser transmitting 2.5 Gbit/s PRBS. The fast detectors were PIN photodiodes (PDT0313) with a bandwidth of 10 GHz and the scope was a 6 GHz digital sampling oscilloscope (Tektronix TDS 820). The fast detectors and detector amplifiers used to measure the signal wave forms are often AC coupled. This causes problems when the frequency chirp is calculated from Eq. (1), since the average power of the signal is also needed. To overcome this problem we used a power meter to track the average power of the signal. The results obtained with this procedure were compared with the result obtained with a DC-connected reference detector (HP 11982A). The wave forms measured with the reference detector were used to calculate the chirp. To avoid errors, the frequency response of the two fast detectors and the amplifiers is required to be the same. A portion of the time traces of a PRBS signal and the corresponding time-resolved frequency chirps are shown in Fig. 6. The signals measured with the real-time chirp analyzer are shown with a solid line. The chirp trace shows that the adiabatic chirp which defines the frequency difference

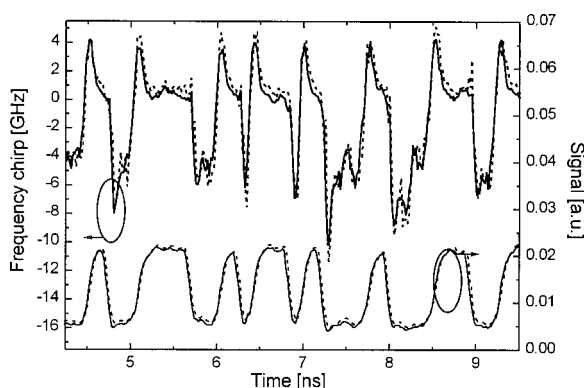


FIG. 6. Traces of the optical signal from the real-time measurement (solid line) and the single etalon measurement (dashed line) and the corresponding time-resolved frequency chirps.

between the 1 and 0 states of the signal is  $\sim 7$  GHz. Transient chirping can be seen as sharp peaks near the leading edge of the signal.

For comparison, the chirp measured with our previous method of using a single etalon is included in the figure (dashed line). The two measurements show similar behavior indicating that the real-time chirp analyzer can reliably be used to characterize optical signals. The actual speed of the real-time measurement is limited only by the averaging performed for the signal and the data acquisition time between the scope and the computer. The chirp trace measured with the real-time chirp analyzer is updated in intervals of less than 1 s.

## VI. DISCUSSION

We have developed and demonstrated a method for measuring time-resolved frequency chirp in real time using two silicon-wafer etalons as frequency discriminators. The accuracy of the chirp analyzer depends primarily on the device used to record the wave form. The noise of the detectors and amplifiers limit the amplitude measurement accuracy at the portions of the signal where the adiabatic chirp is dominating. On the other hand, the accuracy of the measurement of the transient chirp during fast changes of the signal is limited by the time resolution of the etalon which can be improved by employing a thinner etalon. The advantages of this device include insensitivity to the polarization state of light, automated operation and operation over a broad wavelength range. Since the tuning mechanism of the etalon is based on temperature the measurement concept is not sensitive to changes in the ambient temperature. The device can be conveniently used for chirp characterization when the operation parameters of the laser source are varied, since the apparatus does not need repeated initialization. In addition, no DC-connected detectors or amplifiers are needed.

## ACKNOWLEDGMENTS

The authors wish to thank A. Seppänen and F. Desseur for work with the electronics. This work was financially supported by the Academy of Finland, TEKES, and GETA within the ETX program.

- <sup>1</sup>B. Røysted, L. Bjerkan, D. Myhre, and L. Hafskjær, *Electron. Lett.* **30**, 710 (1994).
- <sup>2</sup>F. Devaux, Y. Sorel, and J. F. Kerdiles, *J. Lightwave Technol.* **11**, 1937 (1993).
- <sup>3</sup>A.R. C. Srinivasan and J. C. Cartledge, *IEEE Photonics Technol. Lett.* **7**, 1327 (1995).
- <sup>4</sup>E. Peral, W. K. Marshall, and A. Yariv, *J. Lightwave Technol.* **16**, 1874 (1998).
- <sup>5</sup>R. Linke, *IEEE J. Quantum Electron.* **QE-21**, 593 (1985).
- <sup>6</sup>M. Olesen and H. Olesen, *J. Lightwave Technol.* **9**, 436 (1991).
- <sup>7</sup>W. V. Sorin, K. W. Chang, G. A. Conrad, and P. R. Hernday, *J. Lightwave Technol.* **10**, 787 (1992).
- <sup>8</sup>R. A. Saunders, J. P. King, and I. Hardcastle, *Electron. Lett.* **30**, 1336 (1994).
- <sup>9</sup>R. Monnard, C. R. Doerr, and C. R. Giles, *Proceedings of Optical Fiber Communication (OFC'98)*, OSA Technical Digest Series 1998, Vol. 2, pp. 120–121.

- <sup>10</sup>S. Tammela, H. Ludvigsen, T. Kajava, and M. Kaivola, *IEEE Photonics Technol. Lett.* **9**, 475 (1997).
- <sup>11</sup>T. Niemi, S. Tammela, T. Kajava, M. Kaivola, and H. Ludvigsen, *Micro-wave Opt. Technol. Lett.* **20**, 190 (1999).
- <sup>12</sup>M. Bertolotti, V. Bogdanov, A. Ferrari, A. Jascow, N. Nazarova, A. Pikh-tin, and L. Schirone, *J. Opt. Soc. Am. B* **7**, 918 (1990).
- <sup>13</sup>M. Iodice, G. Cocorullo, F. G. Della Corte, and I. Rendina, *Opt. Commun.* **183**, 415 (2000).